

Quenched carbonaceous composite (QCC) as a carrier of the extended red emission and blue luminescence in the red rectangle

S. Wada¹, Y. Mizutani¹, T. Narisawa², and A.T. Tokunaga³

¹Dept. of Applied Physics and Chemistry, Univ. of Electro-Communications,
Chofugaoka, Chofu, Tokyo 182-8585, Japan
email: wada@pio.jp

²Center for Instrumental Analysis, Univ. of Electro-Communications,
Chofugaoka, Chofu, Tokyo 182-8585, Japan

³Institute for Astronomy, Univ. of Hawaii,
2680 Woodlawn Dr., Honolulu, HI 96822
email: tokunaga@ifa.hawaii.edu

Abstract. Filmy-QCC is an organic material synthesized in the laboratory, and it exhibits red photoluminescence (PL). The peak wavelength of the PL ranges from 650 to 690 nm, depending on the mass distribution of polycyclic aromatic hydrocarbon (PAH) molecules, and the emission profile is a good match for that of the extended red emission in the Red Rectangle nebula. The quantum yield of the PL ranges from 0.009 to 0.04. When filmy-QCC is dissolved in cyclohexane, it exhibits blue PL in the wavelength range of 400–500 nm with a quantum yield of 0.12–0.16. The large width of the red PL and the large wavelength difference between the PL of the filmy-QCC as a solid film and in a solution indicate that there is a strong interaction between the components of filmy-QCC. The major components of filmy-QCC are PAHs up to 500 atomic mass units. Our laboratory data suggest that the blue luminescence observed in the Red Rectangle nebula is probably caused by small PAHs in a gaseous state, and the extended red emission is caused by larger PAHs in dust grains.

Keywords. Methods: laboratory, astrochemistry, (ISM:) planetary nebulae: individual (Red Rectangle), stars: individual (HD44179)

1. Introduction

Extended red emission (ERE), a broad red emission band at 540–950 nm, was first observed in the Red Rectangle (RR) nebula by Cohen *et al.* (1975). ERE of different widths and central wavelengths have been found in reflection nebula, planetary nebula, compact H II regions, and the interstellar medium (see Witt & Vijh 2004 for a review). The ERE arises from photoluminescence. Experiments have shown that various materials emit red luminescence. However, it is thought that a specific class of material gives rise to the ERE. Many candidates for the carrier have been proposed, for example, polycyclic aromatic hydrocarbons (PAHs, d’Hendecourt *et al.* 1986), quenched carbonaceous composite (QCC, Sakata *et al.* 1992), hydrogenated amorphous carbon (HAC, Furton & Witt 1992), carbon clusters (Seahra & Duley 1999), crystalline silicon nanoparticles (Ledoux *et al.* 2001), nanodiamonds (Chang *et al.* 2006), and doubly ionized PAH ions (divalent cations, Witt *et al.* 2006). Koike *et al.* (2002) have also suggested that the ERE is caused by thermoluminescence of silicates.

The RR nebula is illuminated by HD 44179, which is a binary star. The nebula shows many dust features from the ultraviolet to the infrared spectral region, including the infrared emission features (IEF, Sellgren 2001). Recently, blue luminescence (BL) was

detected in the RR by Vijn *et al.* (2004), They suggested small neutral PAHs in the gas phase (three- and four-ring PAHs) could explain the BL.

One hypothesis that we explore here is that the ERE, BL, and IEF arise from related materials. We present in this paper additional experiments on a synthetic dust analog, Quenched Carbonaceous Composite (QCC), and discuss possible carriers of features in the RR.

2. Experiments and Results

Preparation of Filmly-QCC. The preparation method of the filmly-QCC was the same as described in previous papers (Sakata *et al.* 1992, Sakata *et al.* 1994). A schematic of the apparatus and a photograph of it is shown in Figure 1. A. Sakata and co-workers at the University of Electro-Communications designed and built the apparatus to produce QCC. Most of the apparatus was fabricated by themselves. The apparatus was originally made for the study of the formation of molecules observed in the interstellar medium. Polyynes and PAHs are the main products from the plasmic gas (Sakata 1980). However abundant solids were produced from the gas, and it was quickly discovered to have bands similar to that of the IEF.

Two types of material were formed (see Figure 1). One is an organic material (filmly-QCC) and the other is a carbonaceous material (dark-QCC) with onion-like structure (Wada *et al.* 1999). A detailed description of the nature of QCC materials is given by Wada & Tokunaga (2006).

Mass Spectroscopy. Filmly-QCC and dark-QCC were analyzed by a two-step time-of-flight mass spectrometer (TOF-MS) by S. Gillette and T. Mahajan (Stanford University). The samples were heated with a pulsed CO₂ laser, and then the evaporated gases were

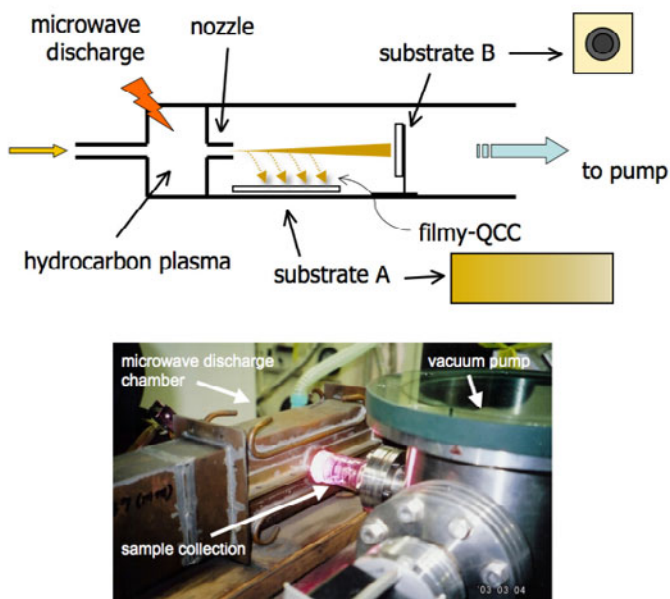


Figure 1. Top: The experimental setup for producing QCC samples. The hydrocarbon plasma is produced in a microwave discharge chamber. The plasmic gas is injected through a small orifice into a vacuum chamber where the QCC sample is collected. Filmly-QCC was collected on a quartz substrate A, located on the wall of the vacuum chamber. Dark-QCC was collected on substrate B, located in the plasmic beam. Bottom: Photograph of the QCC apparatus.

ionized with a YAG laser at a wavelength of 266 nm. C_mH_n peaks of a given carbon number (m) and hydrogen number (n) were detected. Peaks with a different number of hydrogen atoms form a peak group. The central mass of the envelope decreases as the distance of the sampling location from the nozzle increases. The central mass is at 398 atomic mass units (amu) at 5 mm and 252 amu at 70 mm. Larger molecules are therefore formed in the deposit closer to the nozzle. Thus, the major components in the filmy-QCC are compact PAHs.

Two kinds of growth reaction are possible. One is the addition reactions of PAHs to each other, and the other is addition reactions of small radicals to PAH molecules. In the production of both dark-QCC and filmy-QCC, PAH growth is enhanced by high temperature and high density of active species. Schematic diagrams illustrating the structure of the PAH components in the filmy-QCC are presented in Figure 2. The diagrams are based on the mass spectroscopy and analysis of images obtained with a transmission electron microscope (TEM). Curved and parallel structure are often observed in the TEM images of the filmy-QCC (Goto *et al.* 2000). Therefore, we included five-membered carbon rings together with flat PAHs, dihydro-PAHs, and substituted PAHs, and it seems that the PAH molecules are stacked (oriented) locally by intermolecular forces.

Absorption Spectroscopy. Absorption spectra of the filmy-QCCs were measured by a U-3300 UV-VIS spectrophotometer (Hitachi Co). As shown in Figure 3, the absorbance of the filmy-QCC as a solid condensed at 20 and 27 mm from the nozzle has two strong peaks located around 210–230 and 310–320 nm. On the other hand, the absorbance of the samples collected at 5 and 13 mm are composed of two peaks at 220–230 nm and 370–380 nm. Other small absorbance peaks are found in the 400–500 nm region. Thus the filmy-QCC with higher mass PAHs has absorption features at longer wavelengths compared to the filmy-QCC with lighter mass PAHs.

PL of the Filmy-QCC as a Solid and Dissolved in Cyclohexane. We measured the PL spectra of the filmy-QCC with a method similar to that of Sakata *et al.* (1992), and this is shown in Figure 4. The filmy-QCC samples were easily oxidized in air under irradiation of UV. Therefore, we placed them in a vacuum cell and irradiated them with a 365 nm Hg lamp from outside of the cell. The filmy-QCC dissolved in cyclohexane was

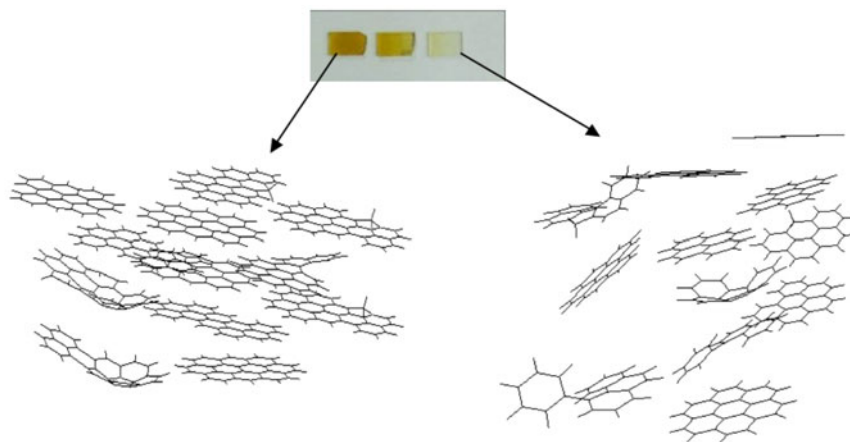


Figure 2. Simplified schematic diagram of the PAH components in the filmy-QCC based on the mass spectroscopy. The material is darker near the nozzle and has larger PAH components (right), compared to the material farther from the nozzle which is lighter in color and has smaller PAH components. Filmy-QCC is a complicated mixture of hydrogenated materials, and this figure does not show all of the components of filmy-QCC.

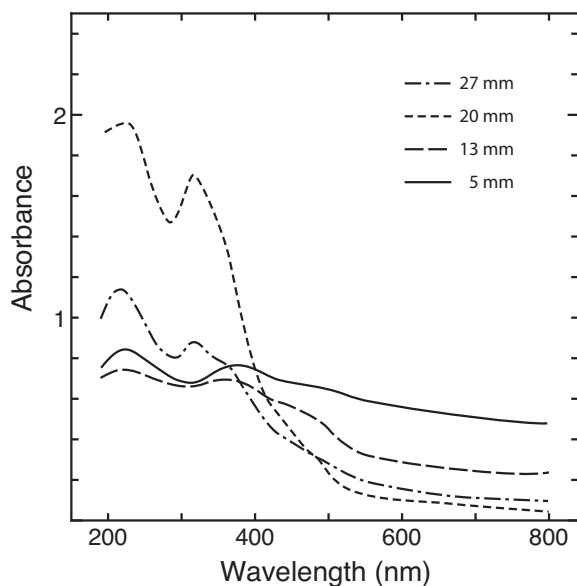


Figure 3. Absorbance spectra of the filmy-QCC, where the absorbance is the quantity $-\log_{10}(\text{transmitted light}/\text{incident light})$. The filmy-QCC was collected on a quartz glass substrate with a length of 40 mm. Spectra were measured using an aperture of 3 mm in diameter at a point along the substrate at 5 mm (solid line), 13 mm (long-dash line), 20 mm (short-dash line), and 27 mm (dot-dash line) from the edge adjacent to the nozzle of the apparatus. These distances correspond to the distance from the nozzle when the QCC was made.

illuminated with a 366 nm deuterium lamp, and the PL was measured with a Hitachi F-4500 fluorescence spectrometer. Dissolved oxygen gas was removed from the cyclohexane before we used it. The filmy-QCC shows PL at 400–500 nm. The PL spectra show a similar trend as with the absorption spectra in that the filmy-QCC with higher mass PAHs has a PL peak at longer wavelengths compared to the filmy-QCC with lighter mass PAHs.

Quantum Yield of the PL. A quantum yield measurement of the PL of filmy-QCC was carried out using films with known quantum yield. We made two standard films with vapor deposition in a vacuum chamber. These were N,N'-diphenyl-N,N'-bis(3-methylphenyl)-1,1'-biphenyl-4,4'-diamine (TPD, quantum yield = 0.35) and N,N'-diphenyl-N,N'-bis(1-naphthylphenyl)-1,1'-biphenyl-4,4'-diamine (NPD, quantum yield = 0.41) (Mattoussi *et al.* 1999). In the case of the filmy-QCC in solution, the quantum yield was obtained by comparison to a standard solution of 9,10-Diphenylanthracene.

The quantum yield of PL is the ratio of the number of luminescence photons to that of the number of photons absorbed, $n(\text{PL})/n(\text{absorbed})$. The quantum yields of the filmy-QCCs are in the range of 0.009–0.04. Quantum yields obtained by the TPD as a standard film are a little smaller than those obtained by the NPD standard. For these measurements, we set up the samples and standard films in the same way. The surface roughness of the films, stray light from the substrate and quartz container, and differences of refractive indices between samples and standard films all have an effect on the measurements. Therefore, we think that the quantum yields of the QCC-films have an accuracy of only one significant figure. Smith & Witt (2002) estimated the photoluminescence efficiency (quantum yield) in various types of astrophysical sources, and they found that it is in the range of 0.1% to 10%.

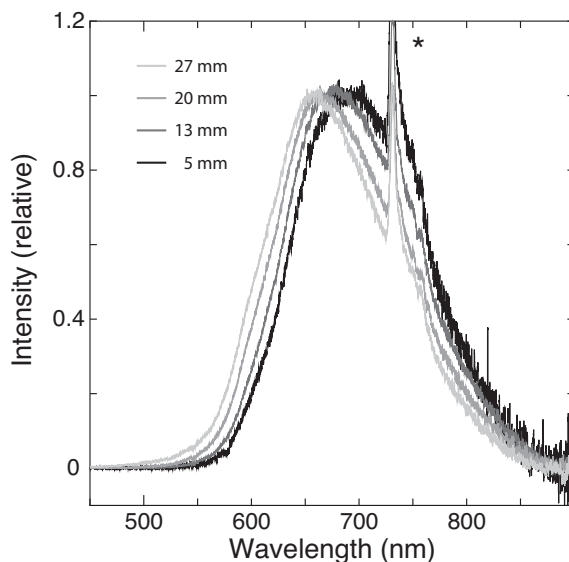


Figure 4. Photoluminescence spectra of the filmy-QCC excited by 365 nm line of the Hg lamp. Samples were collected at 5 mm, 13 mm, 20 mm, and 27 mm from the nozzle (shown from right to left). The spectra are normalized at the peak. An emission line from the Hg lamp is marked with the * symbol.

The quantum yields of the filmy-QCC in the cyclohexane solution are 0.12–0.16. As expected, this is higher than those of the filmy-QCC in the solid state since in the solid form energy is transferred to adjacent molecules. This increases the probability of energy loss through nonradiative processes, thus decreasing the PL yield.

3. Implications for the ERE and BL in the RR

Observational Characteristics of ERE and BL in the RR Nebula. The ERE is clearly observed on the wall of the biconical outflow structure of the RR nebula. In addition, the ladder structure of the RR was also clearly observed with a red filter (Cohen *et al.* 2004). If the red color of the ladder is caused by ERE, the carriers formed before the recent violent outflow event. Cohen *et al.* (2004) reported that the mass loss started about 14,000 yr ago and the outbursts are becoming more frequent.

The peak wavelength of the ERE was observed at the different locations in the RR nebula. Witt & Boroson (1990) found that the peak wavelength varies from ~ 670 nm at $6''$ south of the star to ~ 645 nm at $10''$ south. Ledoux *et al.* (2001), citing the work of Rouan *et al.* (1995), gave a peak wavelength of ~ 755 nm at $2''$ south of the star and ~ 700 nm at $5''$. The FWHM of the ERE peaks is broader as the wavelength of the peak increases. This suggests that the chemical composition, dust structure (arrangement of the molecules), dust size, and physical condition (charge) of the ERE carrier material changes with distance from the central star.

The BL spectrum shows some spectral structure and variability from location to location (Vijh *et al.* 2005), and it is slightly elongated in the east and west direction (Vijh *et al.* 2006). The intensity of the ERE is very strong at the wall of the bipolar outflow, but the BL is distributed around the central region, and the BL and the ERE are not spatially correlated (Vijh *et al.* 2006). Vijh *et al.* (2005) showed that there is a close spatial correlation of the $3.3 \mu\text{m}$ IEF with the BL.

Comparison of ERE and the PL of the Filmy-QCC. Although individual PAHs in the cyclohexane solution show blue-green PL, the mixture in filmy-QCC as a solid shows a red

PL at longer wavelengths. This suggests that there is strong interaction between excited PAHs with neighboring molecules in the solid filmy-QCC material. In our experiments, the PL peak of the filmy-QCCs ranged from 650 to 690 nm with a FWHM of 133–143 nm. From the mass analysis, the peak shift from 650 to 690 nm corresponds to the growth of PAH molecules in the filmy-QCC from 276 to 398 amu at the center mass of the distribution.

The PL peak wavelength of the filmy-QCC depends weakly on the size of molecules. Sakata *et al.* (1992) formed the filmy-QCCs on substrates at a given location with different temperatures. They showed that the PL peak of the sample formed on the higher temperature substrate occurs at longer wavelengths. Thus, the temperature of the substrate is an important factor for growth of PAH molecules. In their experiments, the filmy-QCCs show a peak ranging from 650 to 725 nm.

We show in Figure 5 the ERE spectrum 6'' south from the central binary system of the RR (Witt & Boroson 1990) and a PL of filmy-QCC condensed at 27 mm from the nozzle (central mass peak about 276 amu). The match of the central wavelength and the peak width is very good. We did not find variations of the PL band width of the filmy-QCC. All filmy-QCCs have a similar FWHM. Since the FWHM depends on the mass distribution of PAHs, we think that the right size distribution of PAHs is necessary for good matching to the width of the ERE band observed in the RR.

The PL spectra of filmy-QCC dissolved in cyclohexane overlaps with the spectra of BL. Since the BL peak occurs at a shorter wavelength than what we observe, the BL carriers are smaller PAHs than that of the filmy-QCC components. This supports the idea suggested by Vijh *et al.* (2005) that small PAH molecules in the gas phase are possible BL carriers.

Ionization State of the ERE Carrier. Since PAH molecules have a low ionization potential, we expect that they would be ionized in the biconical outflow cavities of the RR. In general, condensed PAHs possess lower ionization energy than the PAHs in the gaseous state because of the electronic polarization induced by the surrounding molecules. We obtained 5.3 eV for the work function of the filmy-QCC by UV photoelectron spectroscopy with He I. This corresponds to the energy of a photon with a wavelength of 234 nm. However, under irradiation with 172 nm excimer lamp, red emission was also observed

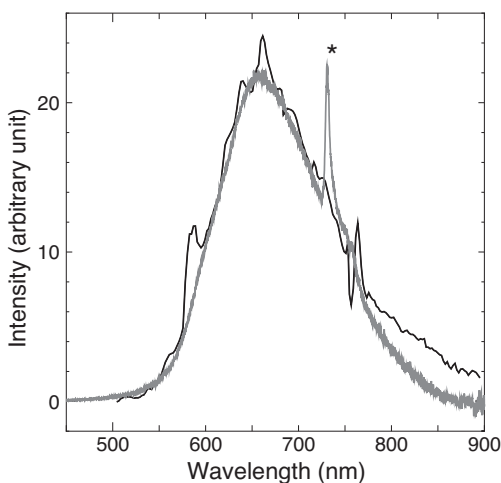


Figure 5. Comparison of the ERE spectrum 6'' south of the RR (black line) from Witt & Boroson (1990) and the PL of the filmy-QCC collected at 27 mm from the nozzle (grey line, see Figure 4). An emission line from the Hg lamp is marked with the * symbol.

clearly by excitation with a 365 nm Hg lamp. The shape of the PL feature does not change by irradiation with a 172 nm lamp. This suggests that neutral PAHs survive under 172 nm irradiation, although some PAHs are ionized. Therefore an important factor is the fraction of neutral PAH molecules in the dust grains that are in the radiation field surrounding the RR.

Decomposition of Dust Particles by UV Irradiation. Under irradiation by hard UV photons, ERE dust grains will gradually decompose because of (1) heating by the UV photons and (2) electrostatic disruption of dust grains due to a high degree of ionization as discussed by Waxman & Draine (2000). Because of the decomposition of the dust grains, isolated PAH molecules and ions are supplied in the outflow cavities. These PAH molecules and ions supplied by dust grains will lose most of their hydrogen atoms. The resulting products with a few hydrogen atoms are not exactly PAHs as defined in chemistry, although their skeletal structure is similar to PAHs. From this viewpoint, they can be considered to be fragments of soot. These products can emit infrared bands when they are heated stochastically, and they could be the IEF carriers. In this scenario, we suspect that the ERE carriers give rise to the IEF carriers through a process of decomposition and dehydrogenation.

4. Conclusions

We obtained the following experimental results about the properties of filmy-QCC:

(a) The major components of the filmy-QCC are PAHs. The sizes were found to be 200–500 amu.

(b) The filmy-QCC shows red PL with a peak wavelength ranging from 650 to 690 nm with a FWHM of 133–143 nm. Our experiments suggest that the PAHs are major emitters of the PL. The PL quantum yield of our filmy-QCC samples ranges from 0.009 to 0.04.

(c) A solution of the filmy-QCC dissolved in cyclohexane shows PL at 400–500 nm with a quantum yield of 0.12–0.16. The large difference in wavelength of the PL peak between the coagulated PAH molecules in filmy-QCC and the dispersed PAH molecules in a solution indicates strong intermolecular interaction of the PAHs with neighboring molecules in the filmy-QCC.

(d) We suggest that ERE emitters are PAHs in dust grains similar composition to the filmy-QCC and BL emitters are small gaseous PAH molecules those do not condense on dust grains.

More details will be presented in a forthcoming paper by Wada, Mizutani, Narisawa, & Tokunaga (in preparation).

Acknowledgements

We thank S. Gillette and T. Mahajan for providing the data shown in Figure 2. S. Wada acknowledges the support of Grant-in-Aid for Scientific Research(C) 17540215. This research has made use of NASA's Astrophysics Data System.

References

- Chang, H.-C., Chen, K., & Kwok, S. 2006, *ApJ* (Letter), 639, L63
Cohen, M., *et al.* 1975, *ApJ*, 196, 179
Cohen, M., Van Winckel, H., Bond, H. E., & Gull, T. R. 2004, *AJ*, 127, 2362
Furton, D. G. & Witt, A. N. 1992, *ApJ*, 386, 587
d'Hendecourt, L. B., Léger, A., Olofsson, G., & Schmidt, W. 1986, *A&A*, 170, 91
Goto, M., Maihara, T., Terada, H., Kaito, C., Kimura, S., & Wada, S. 2000, *A&AS*, 141, 149
Koike, K., Nakagawa, M., Koike, C., Okada, M., & Chihara, H. 2002, *A&A*, 390, 1133

- Ledoux, G., Guillois, O., Huisken, F., Kohn, B., Porterat, D., & Reynaud, C. 2001, *A&A*, 377, 707
- Mattoussi, H., Murata, H., Merritt, C. D., Iizumi, Y., Kido, J., & Kafafi, Z. H. 1999, *J. Appl. Phys.*, 86, 2642
- Rouan, D., Lecoupanec, P., & Léger, A. 1995, in: C. S. Jeffery (ed.), *Proc. 1st Franco-British meeting on the Physics and Chemistry of the Interstellar Medium, Newsletter on Analysis of Astronomical Spectra, no. 22*, p. 37
- Sakata, A. 1980, in: B.H. Andrew (ed.), *Interstellar Molecules, IAU Symp 87*, (Dredrecht: Reidel), p. 325
- Sakata, A., Wada, S., Narisawa, T., Asano, Y., Iijima, Y., Onaka, T., & Tokunaga, A. T. 1992, *ApJ* (Letter), 393, L83
- Sakata, A., Wada, S., Tokunaga, A. T., Narisawa, T., Nakagawa, H., & Ono, H. 1994, *ApJ*, 430, 311
- Seahra, S. S. & Duley, W. W. 1999, *ApJ*, 520, 719
- Sellgren, K. 2001, *Spectrochimica Acta*, 57, 627
- Smith, T. L. & Witt, A. N. 2002, *ApJ*, 565, 304
- Vijh, U. P., Witt, A. N., & Gordon, K. D. 2004, *ApJ* (Letter), 606, L65
- Vijh, U. P., Witt, A. N., & Gordon, K. D. 2005, *ApJ*, 619, 368
- Vijh, U. P., Witt, A. N., York, D. G., Dwarkadas, V. V., Woodgate, B. E., & Palunas, P. 2006, *ApJ*, 653, 1336
- Wada, S., Kaito, C., Kimura, S., Ono, H., & Tokunaga, A. T. 1999, *A&A*, 345, 259
- Wada, S., & Tokunaga, A. T. 2006, in: F. J. M. Rietmeijer (ed.), *Natural Fullerenes and Related Structures of Elemental Carbon*, (Dordrecht: Springer), p. 31
- Waxman, E., & Draine, B. T. 2000, *ApJ*, 537, 796
- Witt, A. N., & Boroson, T. A. 1990, *ApJ*, 355, 182
- Witt, A. N., Gordon, K. D., Vijh, U. P., Sell, P. H., Smith, T. L., & Xie, R.-H. 2006, *ApJ*, 636, 303
- Witt, A. N. & Vijh, U. P. 2004, in: A. N. Witt, G. C. Clayton, & B. T. Draine (eds.), *ASP Conf. Ser. 309, Astrophysics of Dust*, (San Francisco: ASP), p. 115

Discussion

SLOAN: I remember quite a while ago that Adolf Witt had imaged the extended red emission in the Red Rectangle to be in a big X shape along the edges of the conical cavities north and south of the central star. If that is the case, then it seems to me that the carriers of the extended red emission are not newly formed grains, but are grains that haven't been destroyed yet because they are at the edge of the destruction zone.

HENNING: I think the structure is still the same; the interpretation is another question of course.

MULAS: I have simple technical question and another one about the Red Rectangle. The technical question – You showed how the photoluminescence spectrum of your samples changes with properties of the sample and you also showed the geometry with which you collect the light. Since emitted light has to travel some distance inside your sample before getting out, it probably undergoes some self-absorption. Did you compensate your spectrum for that? As your samples become more absorbing they may change the spectrum just due to that. About the Red Rectangle - It looks like it could be a problem to explain the luminescence by very small PAHs because you would have those very few PAHs, because they are so small and are very highly excited by every single photon, emitting more at 3.3 μm than you actually see. That may be a bit of the problem with the observations.